Decomposition of the Metastable Beta Phase in the All-Beta Alloy Ti-13V-11Cr-3Al

G. HARI NARAYANAN and T. F. ARCHBOLD

The phase transformations which occur in the all-β titanium alloy Ti-13V-11Cr-3Al at temperatures below ~500°C have been studied by transmission electron microscopy, X-ray diffraction, and electrical resistivity techniques. The decomposition of the metastable β phase has been found to proceed through a transition reaction leading to the formation of two bcc phases rather than through the precipitation of the ω phase as has been previously reported. An interpretation of the observed decomposition sequence, based on thermodynamic reasoning, is presented. The decomposition characteristics of the Ti-13V-11Cr-3Al alloy have been compared with those of a Ti-13V-11Cr alloy to determine the influence of aluminum on the transformation behavior.

THE phase transformations which occur during the athermal and isothermal decomposition of the metastable bcc or β phase in several β-stabilized titanium alloys have received considerable attention in the past two decades. The different modes of the decomposition of the supersaturated β phase observed in a variety of titanium alloys have been discussed in detail by McQuillan,[1] Bagariatskii,[2] and more recently by Blackburn and Williams.[3] The work described in this paper is concerned with the phase transformation behavior of the all-β titanium alloy Ti-13V-11Cr-3Al, commercially known as B120VCA. This alloy contains a substantially high amount of β-stabilizers which make the β decomposition reactions extremely sluggish; thus, β can be retained at room temperature even after furnace cooling. The preliminary report on this alloy by Wood and Ogden[4] shows that the high vanadium content of the alloy, although it makes a significant contribution to the stabilization of the β phase, does not influence the Ti-Cr eutectoid reaction. However, the investigations by Imgram *et al.*[5] of several β-Ti alloys containing vanadium, chromium, and aluminum, indicate that increasing additions of vanadium tend to soften the material during aging treatments through a tendency for increased rejection of the intermediate phase $TiCr_2$. Aluminum, which is an α stabilizer, has been shown to improve the aging response of the alloy by shifting the aging characteristics to those observed in low-chromium ternary alloys.[4,5] The present alloy, therefore, behaves like a hypoeutectoidal Ti-Cr alloy in many respects.

Earlier investigations of the isothermal aging characteristics of the Ti-13-11-3 alloy[4,6-8] suggest that the decomposition of the metastable β phase at temperatures in the range 300° to 500°C proceeds through the formation of the transition phase ω, as has been observed in several β stabilized binary and ternary titanium alloys. The evidence presented in these studies was based mainly on optical metallography and X-ray analysis and was inadequate for the positive identification of the ω phase. Attempts to resolve this problem by use of replica techniques[9] did not yield further useful information. Consequently, the reaction sequence during the decomposition of the metastable β phase in this temperature range has been believed to be:

$$\beta_m \rightarrow \beta_\gamma + \omega \rightarrow \beta_\gamma + \omega + \alpha \rightarrow \beta_\gamma + \alpha \rightarrow \beta_e + \alpha + TiCr_2$$

where β_m, β_γ and, β_e refer to the metastable, enriched, and equilibrium β phases, respectively.

In the present studies, the authors have examined this reaction sequence using transmission electron microscopy, X-ray diffraction analysis, electrical resistivity, and hardness measurement techniques.

EXPERIMENTAL PROCEDURE

The Ti-13V-11Cr-3Al alloy was received in the form of mill annealed, 0.045 in. thick sheet. The composition in weight percent of the as-received material was: 13.2 pct V, 11.2 pct Cr, 3.15 pct Al, 0.19 pct Fe, 51 ppm N_2, 97 ppm H_2, and 1090 ppm O_2. Strips cut from the sheet were vacuum annealed at 850° C for approximately 4 hr and cold rolled to a thickness of 0.015 in. Specimens in the form of coupons were prepared from rolled material and solution treated at 800°C for $1\frac{1}{2}$ hr in purified helium using titanium foil as a "getter." Solution treated specimens were quenched in water, oil, or air in order to examine the effect of cooling rate on subsequent aging reactions. A number of specimens were solution treated at 900°C and water quenched so as to study the effect of the solution treatment temperature. Aging was done in salt baths held at temperatures in the range 250° to 500°C for times exceeding 1000 hr. A few specimens were deformed 5, 10, and 15 pct in compression prior to aging in order to examine the influence of cold work on aging characteristics.

In order to investigate the role of aluminum in the decomposition reactions of the metastable β, a ternary titanium alloy containing 13 pct V and 11 pct Cr was prepared by arc melting in a purified helium atmosphere. The as-cast material was homogenized at 850°C for 24 hr in vacuum and cold rolled into 0.015 in. thick strips. The rolled alloy contained 860 ppm O_2 and 122 ppm H_2. Heat treatment procedures were identical to those given to Ti-13V-11Cr-3Al alloy specimens.

Thin foils for transmission electron microscopy

G. HARI NARAYANAN and T. F. ARCHBOLD are Predoctoral Research Associate and Associate Professor, respectively, Division of Metallurgical Engineering, University of Washington, Seattle, Wash.

Manuscript submitted October 1, 1969.

were prepared using a modified Bollman technique[10] with the operating conditions prescribed by Blackburn and Williams[11] to avoid hydrogen contamination.

Needle specimens for Debye-Scherrer X-ray diffraction experiments were prepared from both the bulk and the thin foil material. All X-ray samples were chemically polished following heat treatments, using a solution of 2 parts of HNO_3 and 1 part HF cooled by liquid nitrogen. Lattice parameter measurements of the β phase were made with the aid of a 114.6 mm camera using Cu-K_α radiation. Step scanning over selected β-phase reflections was performed on flat bulk samples with a Siemens X-ray diffractometer unit. Changes in electrical resistances during isothermal aging treatments were measured at −196°C using rod samples approximately 3 in. long and 0.075 by 0.05 in. in cross section.

RESULTS

A) Electron Microscopy

Spontaneous transformation was found to occur during thin foil preparation of almost all of the Ti-13V-11Cr-3Al and Ti-13V-11Cr specimens. A similar phenomenon has been reported for several binary titanium alloys[3,12] and a few commercial alloys.[13] The origin of this transformation and the details of the structure and morphology of the transformation products have been discussed elsewhere.[3,14] The spontaneous transformation not only complicates the analysis of other structures present, but also poses problems in thin foil preparation through its embrittling effect. In order to eliminate the influence of spontaneous transformation on subsequent interpretations, all electron diffraction observations were made in thicker regions of the foils where this transformation was absent.

In the as-quenched condition the Ti-13V-11Cr-3Al alloy has a single phase structure with varying amounts of the spontaneous transformation product being present along the thinner regions of the foil. No evidence of the transition phase ω could be detected in the as-quenched and aged condition either from the electron diffraction patterns or from the electron micrographs. However, after aging for short periods of time at temperatures below 500°C, a fine precipitate was observed to be dispersed throughout the matrix. The precipitate particles attained a size of approximately 150Å after aging for 75 hr at 250°C, Fig. 1. Considerably less time was required for the particles to attain a detectable size during aging at the higher temperatures, Fig. 2.

The Ti-13V-11Cr alloy specimens, in addition to the spontaneous transformation along the thin regions, exhibited the presence of an extremely fine dispersion of particles in the as-quenched condition, Fig. 3. No additional reflections which could be attributed to a second phase were present in the electron diffraction patterns, thus discounting the possibility that these particles could be quenched-in ω, Fig. 4. The influence of the aging temperature on the size and distribution of these particles and the sequence of their growth with time at any fixed aging temperature were identical to those observed in the Ti-13V-11Cr-3Al alloy.

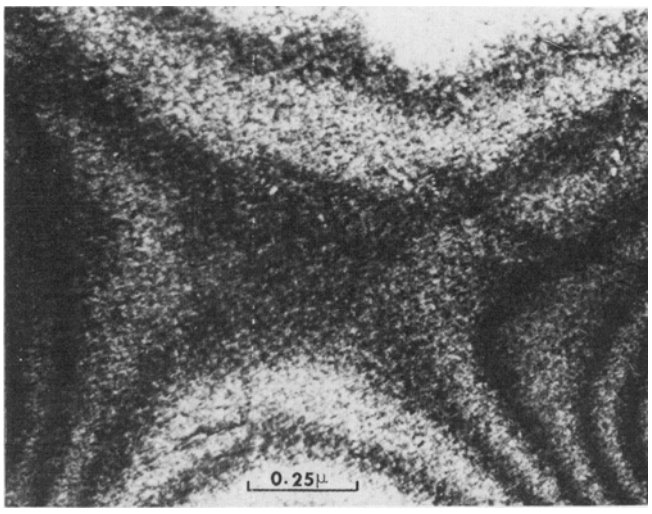

Fig. 1—Bright field electron micrograph showing the fine dispersion of precipitates in Ti-13V-11Cr-3Al alloy following solution treatment at 800°C, water quench, and aging for 75 hr at 250°C. $\langle 111 \rangle_\beta$ zone normal.

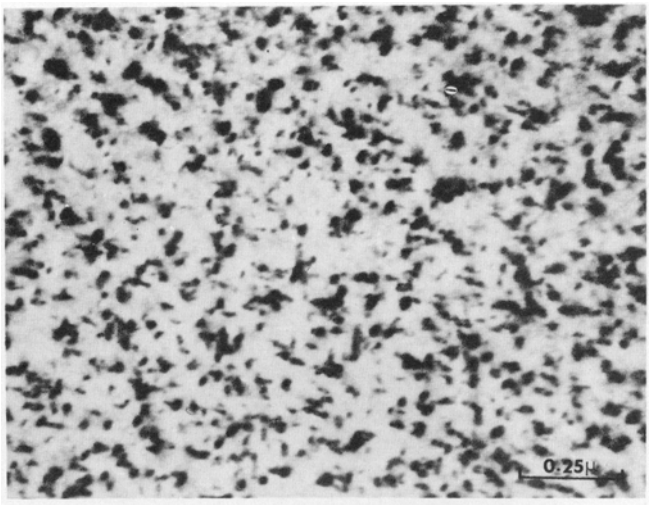

Fig. 2—Bright field electron micrograph from the Ti-13V-11Cr-3Al alloy aged at 350°C for 25 hr following solution treatment at 800°C and water quench. $\langle 111 \rangle_\beta$ zone normal.

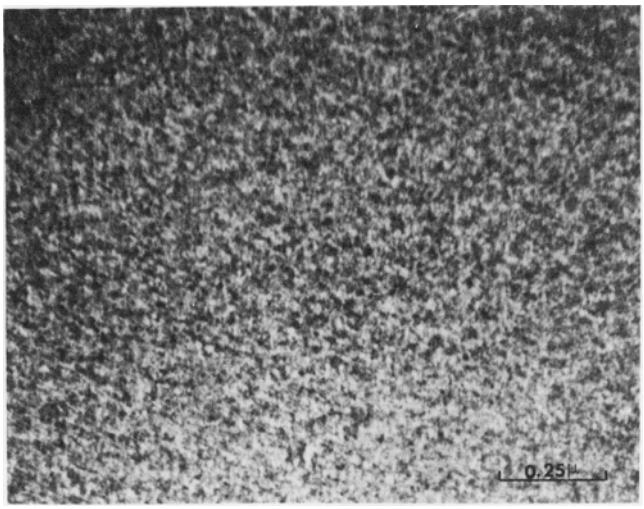

Fig. 3—Bright field electron micrograph from the Ti-13V-11Cr alloy, water quench following solution treatment at 800°C. $\langle 120 \rangle_\beta$ zone normal.

It was difficult to discern the shapes of these particles during the early stages of their growth; generally, they appeared as equiaxed particles. At higher aging temperatures or after prolonged aging at lower temperatures, the particles were approximately disc shaped or plate-like, with three distinct orientations, Figs. 5 and 6. Trace analysis has shown that the discs lie approximately parallel to the $\{100\}$ planes of the bcc matrix, Fig. 6. The appearance of displacement fringes, Fig. 7, and 'dislocation ring' contrast, Fig. 11 *a*, indicates that some coherency exists between the precipitates and the matrix. The present observation, Fig. 6, of the black-to-white contrast changes associated with precipitate discs which lie parallel to the incident beam is insufficient[15] for a conclusive determination of the nature of the elastic displacements.

Selected area diffraction patterns taken from regions containing appreciable amounts of the precipitate show only β-phase reflections and no additional spots due to a second phase in both Ti-13V-11Cr-3Al and Ti-13V-11Cr alloys, Fig. 8. However, the matrix spots themselves were split; this splitting was more pronounced for higher-order reflections. The streak directions in Fig. 8 are inconsistent with the particle shape effects expected from thin discs parallel to $\{100\}$. Since the observed streaks do not pass through the origin of the reciprocal lattice, and they are asymmetric about each spot, it is concluded that the streaks are due to coherency strains. Very diffuse streaking, Fig. 4, with no apparent maxima constituted a background to the diffraction patterns. The nature of this diffuse intensity network was characteristic of the zone being examined; these streaks are along $\langle 110 \rangle$ directions in $\langle 100 \rangle_\beta$ and $\langle 111 \rangle_\beta$ zone patterns and along $\langle 112 \rangle$ directions in a $\langle 110 \rangle_\beta$ zone pattern. The diffuse network is attributed to coherency strain effects in view of the absence of the expected particle shape effects.

Since the only observable feature of the electron diffraction patterns, apart from the diffuse streaking, which could be associated with the unidentified precipitates was the splitting of the matrix spots, it was assumed that the precipitates have the same structure as the parent phase. This implies that the matrix and the precipitate differ only in their '*d*' spacings, and therefore in composition. Thomas[16] and van Torne and Thomas[17] have shown that Kikuchi line analysis can be applied to the study of phase transformations involving clustering or spinodal decomposition. They suggest this analysis as the only means to detect localized compositional variations occurring over relatively short distances in a solid solution. A Kikuchi line analysis was performed on the present samples which contain the unidentified precipitate. Kikuchi lines were found to be paired, Fig. 9, as would be expected from a system in which solute segregation has occurred. The pairing of the Kikuchi lines was observed for all specimens which had been heat treated to produce the precipitate, in both Ti-13V-11Cr-3Al and Ti-13V-11Cr alloys.

When the '*d*' spacings of the precipitate and parent phases are nearly the same, the precipitate and matrix reflections often coincide in a normal diffraction pattern, and hence the precipitate reflections may not be resolvable. However, the precipitates themselves may be revealed by forming dark field images of a common reflection. Better resolution is obtained under a two beam situation where the beam is tilted so as to bring the negative of the operating reflection along the optic axis.[16] Dark field examination showed the precipitate

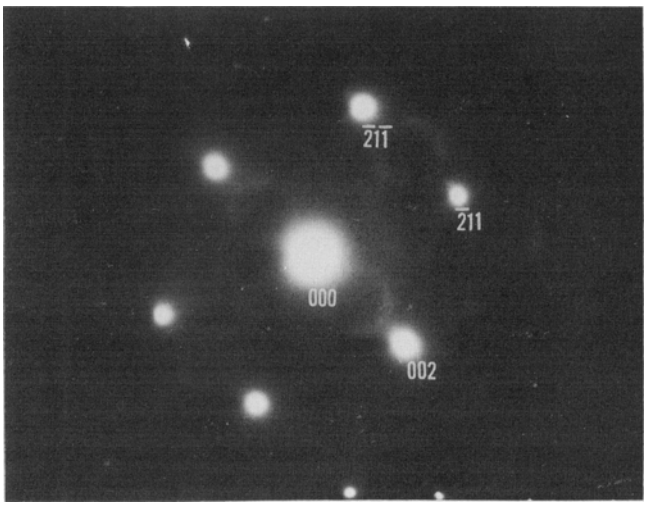

Fig. 4—Selected area diffraction pattern from the general area corresponding to the micrograph in Fig. 3. $\langle 120 \rangle_\beta$ zone normal.

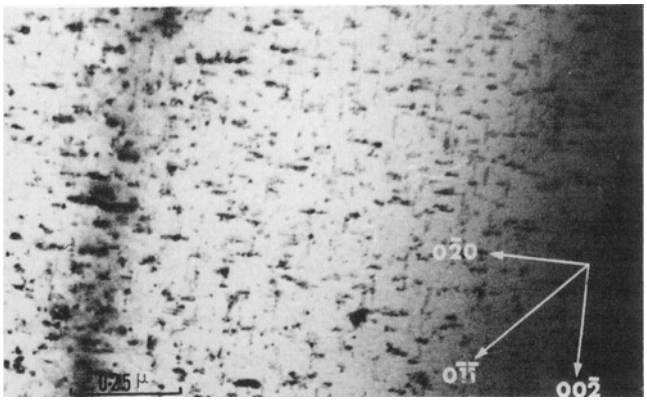

(*a*)

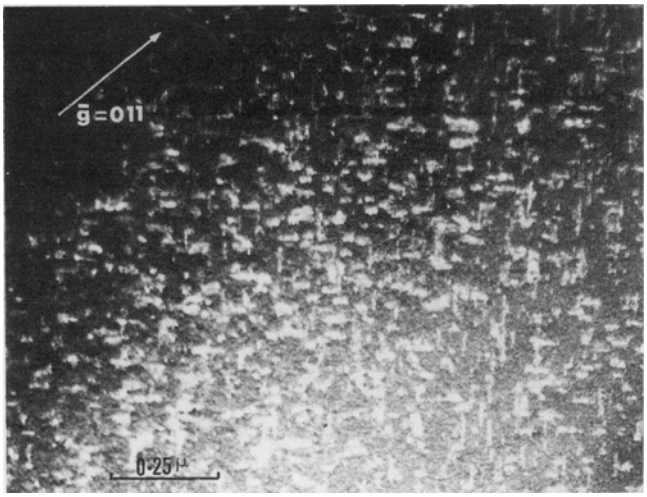

(*b*)

Fig. 5—(*a*) Bright field electron micrograph showing the distribution of precipitates in the Ti-13V-11Cr-3Al alloy aged at 400°C for 6 hr following solution treatment at 1050°C and air cooling. $\langle 100 \rangle_\beta$ zone normal. (*b*) Dark field micrograph corresponding to the area in Fig. 5(*a*).

particles to be clearly resolved as illustrated in Fig. 5 (*b*). The symbol β_2 will be used to designate this precipitate in the remainder of this paper.

The presence of precipitate free zones adjacent to the β grain boundaries, Fig. 10, suggests that a vacancy mechanism must be responsible for the nucleation and growth of the β_2 particles. In order to examine further the role of vacancies in the formation of β_2, additional coupons were cooled at various rates from 800°, 900°, or 1050°C. All specimens were then aged at 400°C for 6 hr to produce the β_2 precipitate. The size and distribution of β_2 are influenced strongly by the solution treatment temperature and the subsequent cooling rate. Specimens quenched from a higher solution treatment temperature exhibit smaller precipitates, Fig. 11 (*a*) and (*b*). Also, for a given solution treatment temperature, smaller precipitates, Fig. 11 (*a*), (*c*), and (*d*), and narrower precipitate free zones, Fig. 11 (*e*) and (*f*), are observed for the faster cooling rates.

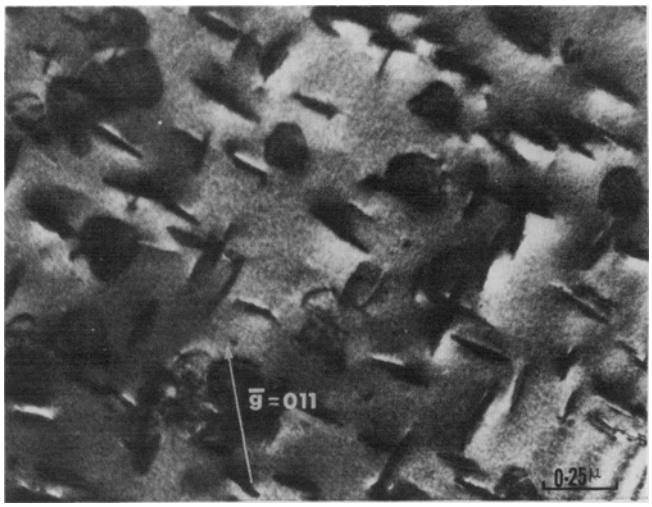

Fig. 6—Dark field electron micrograph taken from the (011) matrix reflection for Ti-13V-11Cr alloy aged for 24 hr at 400° C following solution treatment at 800°C and water quench. Close to $\langle 100 \rangle_\beta$ zone normal.

Fig. 7—Bright field electron micrographs illustrating the displacement fringes observed when the specimen was tilted from the orientation corresponding to Fig. 6.

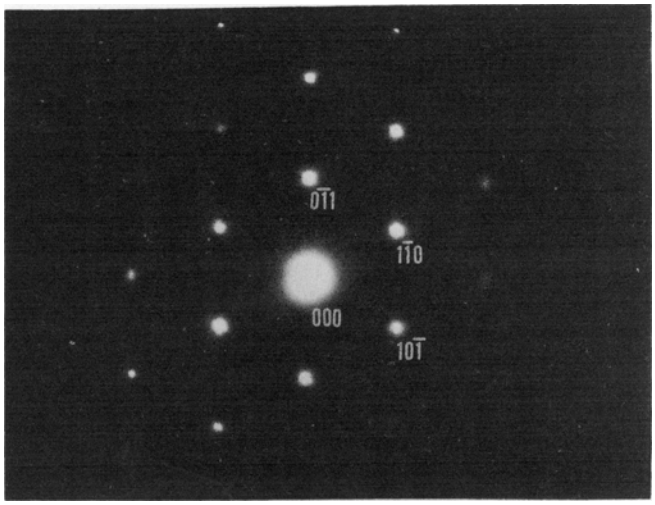

Fig. 8—Selected area diffraction pattern taken from Ti-13V-11Cr-3Al alloy aged at 400°C for 6 hr following solution treatment at 800°C and water quench. The matrix reflections are split and diffuse streaks lie along $\langle 110 \rangle$ directions. $\langle 111 \rangle_\beta$ zone normal.

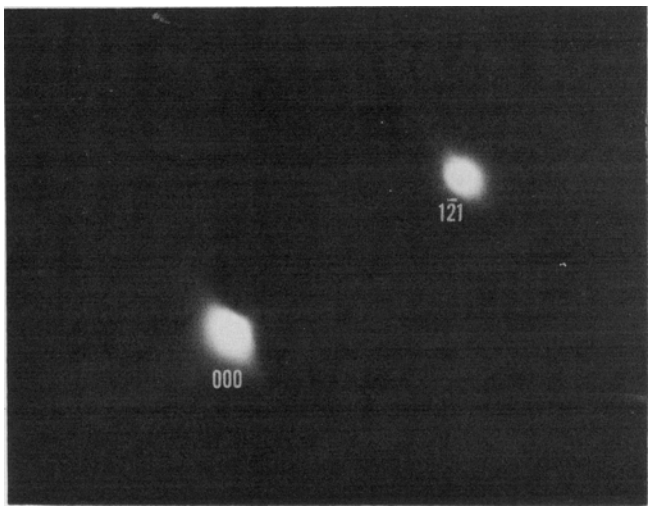

Fig. 9—Selected area diffraction pattern showing the pairing of the Kikuchi lines in Ti-13V-11Cr-3Al alloy aged for 6 hr at 400°C following solution treatment at 800°C. Close to $[111]_\beta$ zone normal.

A similar range in the size and distribution of β_2 was observed with variations in the aging temperature, with the precipitate being smaller after aging at the lower temperatures. For a particular heat treatment procedure, the volume fraction of the β_2 precipitates present was higher for the ternary alloy as compared with the quarternary alloy in which aluminum was present.

Although a preferential nucleation on dislocations was observed in a few specimens, Fig. 12, the β_2 precipitates in general show little tendency for heterogeneous nucleation. This has been confirmed by examining the aging kinetics of Ti-13V-11Cr-3Al alloy specimens which were deformed 5, 10, and 15 pct by rolling prior to aging. The incubation period for precipitation of the α phase was reduced appreciably by cold work prior to aging, while there was little influence on the precipitation kinetics of the β_2 phase.

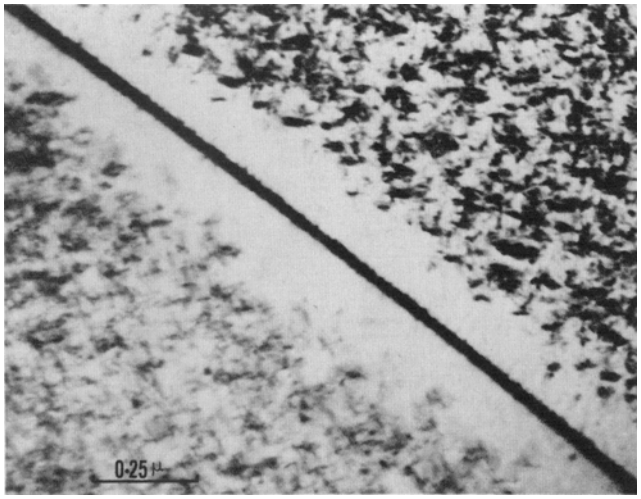

Fig. 10—Bright field electron micrograph showing the precipitate free zone adjacent to a β-grain boundary in Ti-13V-11Cr-3Al alloy, solution treated at 800°C, water quenched, and aged at 400°C for 10 hr.

The stability of the β_2 phase was examined by conducting reversion experiments. Ti-13V-11Cr-3Al specimens, water quenched from the solution treatment temperature, were first aged at 400°C for 6, 10, or 18 hr and then reheated to 550°, 600°, or 800°C for times up to 3 hr. In samples reheated to 550°C the precipitation of the α phase started prior to the completion of the redissolution of β_2 particles. At 600° and 800°C, on the other hand, reheating for a period less than 3 hr was adequate to cause complete reversion of the β_2 phase.

Prolonged aging at all temperatures resulted in the growth of the β_2 particles to consume a major portion of the matrix before the precipitation of the α phase begins. For the Ti-13V-11Cr-3Al alloy specimens, the precipitation of α could be first detected only after aging at 300°C for periods up to approximately 250 hr; the α phase appeared after approximately 10 hr of aging at 450°C. The precipitation of the α phase was retarded considerably in the ternary alloy Ti-13V-11Cr. The presence of the α precipitate could be detected only after aging for approximately 100 hr at 400°C as

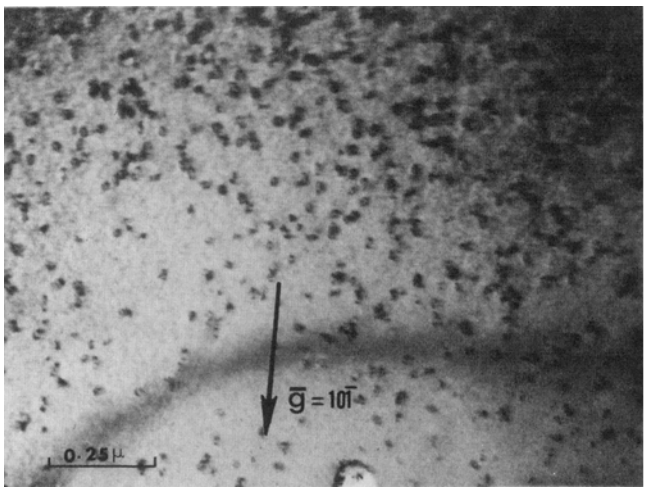

(a)

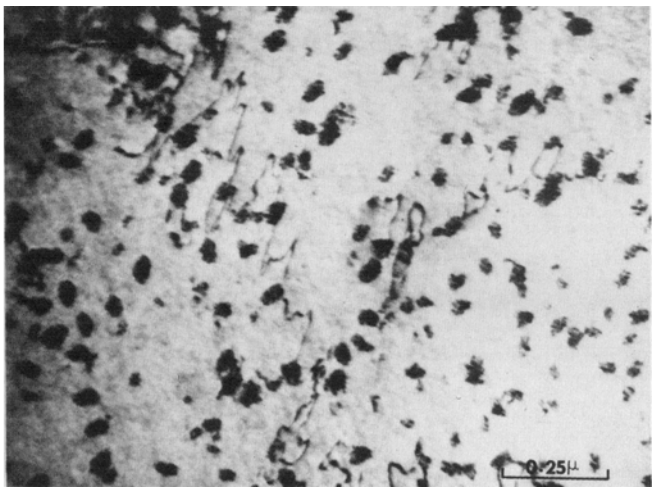

(c)

(b)

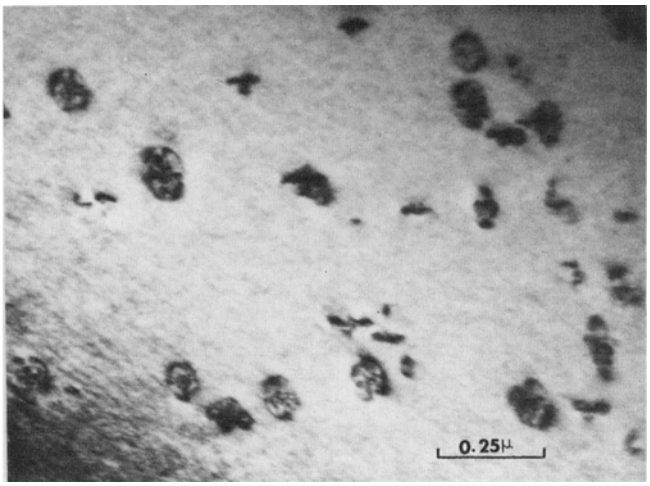

(d)

Fig. 11—Electron micrograph showing the size and distribution of the precipitates and width of precipitate free zones as a function of heat-treatment variables. (*a*) Solution treated at 800°C, water quenched, and aged at 400°C for 6 hr. (*b*) Solution treated at 900°C, water quenched, and aged at 400°C for 6 hr. (*c*) Solution treated at 800°C, oil quenched, and aged at 400°C for 6 hr. (*d*) Solution treated at 800°C, air cooled, and aged at 400°C for 6 hr. (*e*) Solution treated at 1050°C, brine quenched, and aged at 400°C for 6 hr. (*f*) Solution treated at 1050°C, air cooled, and aged at 400°C for 6 hr, also see Fig. 5(*a*), (*b*).

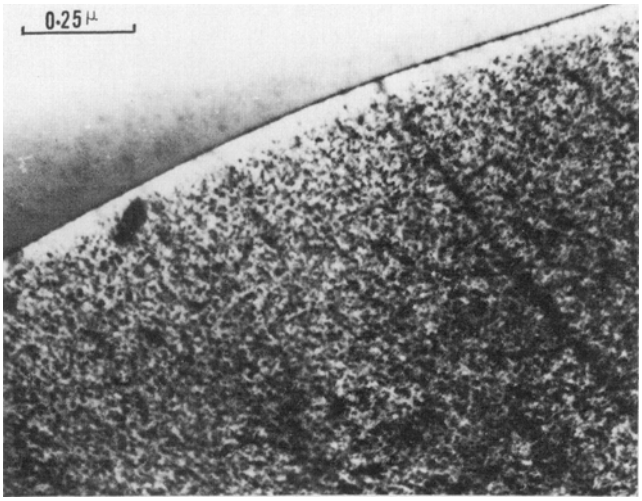

Fig. 11–Continued. (e)

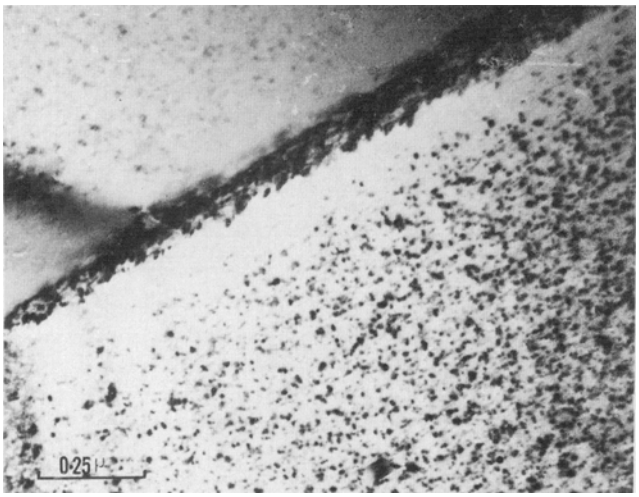

(f)

compared to the 25 hr required to produce α in the quarternary alloy at the same aging temperature.

The precipitation of the α phase initiates simultaneously at the grain boundaries and within the grains, although grain boundary regions appear to be preferred nucleation sites, Fig. 13. In samples of the Ti-13V-11Cr-3Al alloy aged at 350°, 400°, or 450°C, it was observed that the nucleation of the α phase within a grain occurs near the interfaces between β_2 and the matrix or in regions between β_2 particles, Fig. 14. The α precipitates are needle shaped, and they exhibit a Widmanstätten morphology with their needle axes lying along $\langle 110 \rangle_\beta$ directions, Fig. 15.

The hcp structure of the α phase was confirmed by electron diffraction, Fig. 16, and X-ray diffraction analysis. The orientation relationship between the α and the β phases was found to be the expected Burgers' relation:

$$(110)_\beta // (0001)_\alpha$$
$$[\bar{1}11]_\beta // [11\bar{2}0]_\alpha$$

B) X-ray Diffraction Studies

Harmon and Troiano[18] proposed that the decomposition of the metastable β in Ti-16 pct V-2.5 pct Al and Ti-20 pct V alloys at temperatures below 270°C proceeds through a phase separation reaction leading to the formation of solute rich and solute lean bcc phases. The evidence for such a reaction was the splitting of the β-phase reflections into sharp components. In the present investigations the β-peak splitting was examined using step scanning over selected higher angle reflections. Although splitting was observed in some cases, no reproducible results were obtained. The β-phase reflections became too broad and diffuse, particularly for specimens aged for short periods of time at temperatures between 300° and 450°C. Similar blurring of the higher angle β reflections has been reported by Ageyev and Novik[19] in the aged β alloy Ti-9Mo-7Mn containing 1 to 2 pct Al, and also by Blackburn and Williams[3] in a Ti-20 pct V alloy after aging for 100 hr at 200°C.

The method of graphical extrapolation was used to determine the changes in the lattice parameter of the

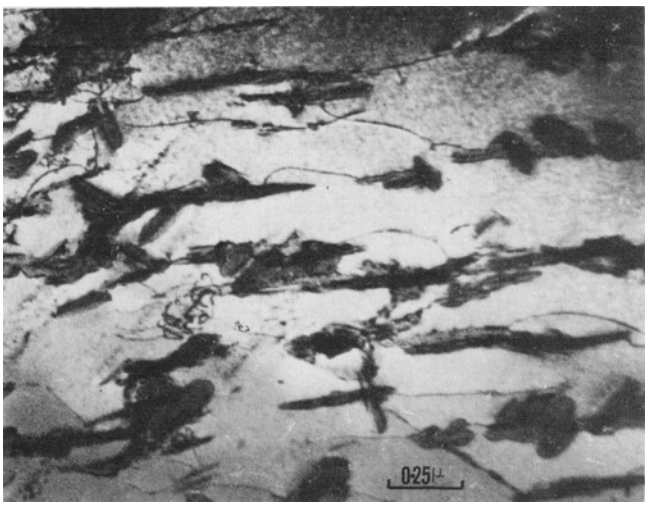

Fig. 12—Bright field electron micrograph from Ti-13V-11Cr-3Al alloy aged at 500°C for 2 hr following solution treatment at 800°C and water quench, showing the precipitation of β_2 phase on dislocations.

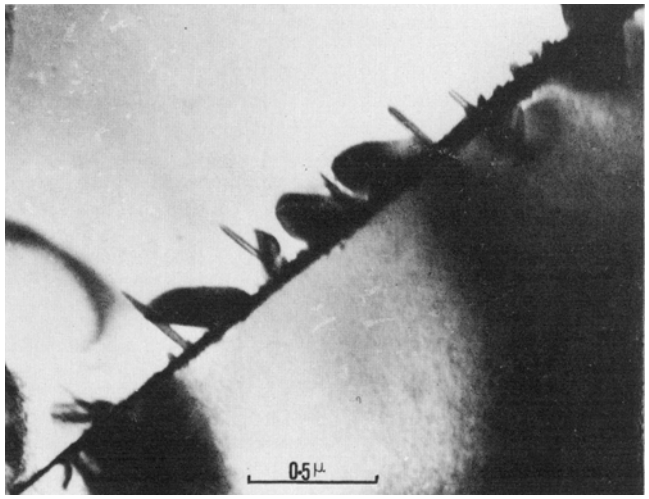

Fig. 13—Bright field micrograph showing the nucleation of α phase on the grain boundary in Ti-13V-11Cr-3Al alloy aged at 500°C for 4 hr following solution treatment at 800°C and water quench.

retained β phase in the Ti-13V-11Cr-3Al alloy as a function of time during isothermal treatments at temperatures between 300° and 500°C. Only the first five reflections in the low angle regions were used since the higher angle reflections were too blurred to make precise measurements. The lattice parameter shows an increase during the early stages of the decomposition at each of the temperatures, and this increase is followed by rapid decrease, Fig. 17. Isothermal aging at 400°C of the ternary alloy Ti-13V-11Cr exhibited a similar behavior. It is interesting to note that the dilatometric data presented by Harmon and Troiano[18] was characterized by an initial expansion followed by a contraction in volume. They attributed this peak effect to the onset of the $\beta_m \rightarrow \beta_{rich} + \beta_{lean}$ reaction.

The application of the X-ray diffuse scattering techniques to yield a quantitative measure of local order will be of little assistance in the case of Ti-V-Cr alloys because of the similar atomic scattering factors for these elements. Hence, no attempt was made to measure local compositional variations using this technique.

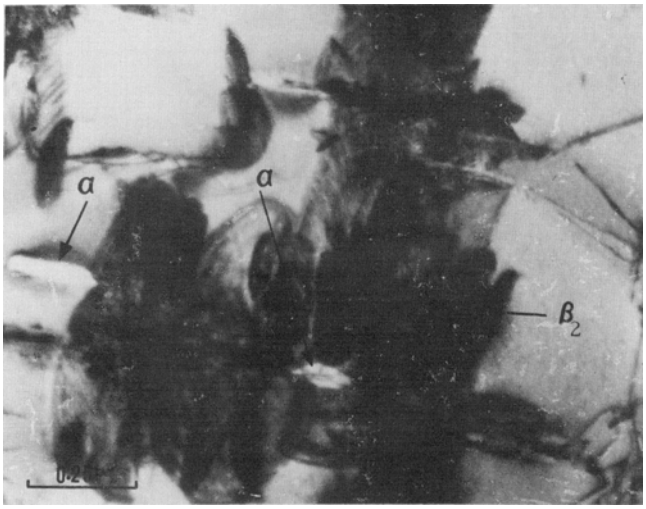

Fig. 14—Electron micrograph showing the nucleation of the α phase at the β_2-matrix interface in the Ti-13V-11Cr-3Al alloy aged at 450°C for 10 hr following solution treatment at 800°C and water quench.

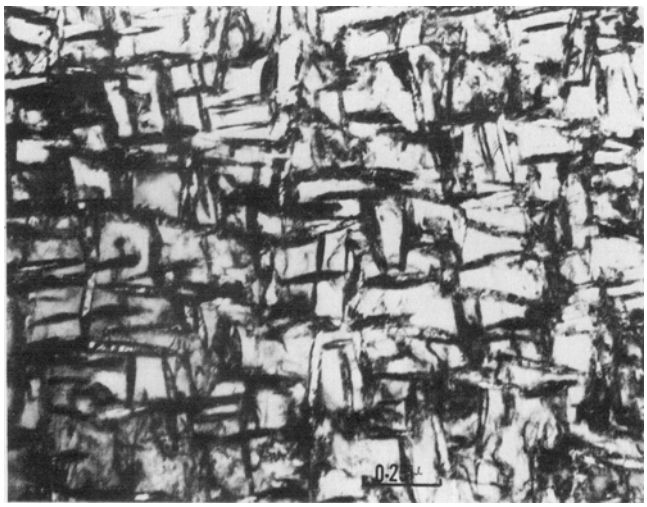

Fig. 15—Widmanstätten morphology of the α-phase precipitates in Ti-13V-11Cr-3Al alloy aged at 400°C for 350 hr. $\langle 100 \rangle_\beta$ zone normal.

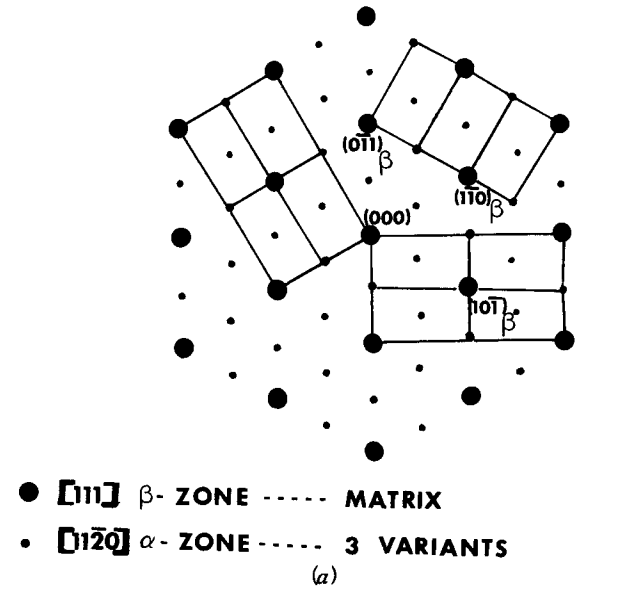

(a)

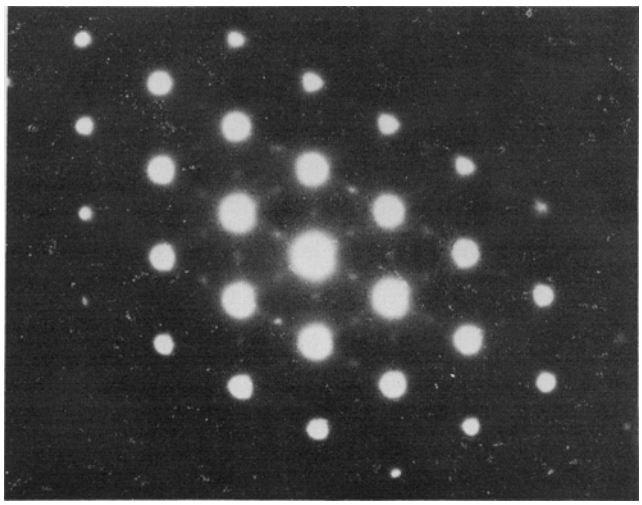

(b)

Fig. 16—Selected area diffraction pattern from Ti-13V-11Cr-3Al alloy aged at 300°C for 1000 hr showing the superimposed patterns from β and α phases.

C) Electrical Resistivity Measurements

Changes in electrical resistivity have been used as a successful tool to follow clustering reactions and zone formation.[20,21] As clusters form, the electrical resistivity rises to a maximum and then decreases. There is evidence that this resistivity peak is related to a characteristic state of the alloy which is the same irrespective of the aging temperature.[21,22]

Resistivity changes were measured during isothermal aging experiments at 300°, 350°, and 400°C in the Ti-13V-11Cr-3Al alloy. At each of the three temperatures, the resistivity of the samples increased above the as-quenched value during the early stages of isothermal aging. The resistivity change remained positive until the initiation of the precipitation of the α phase, Fig. 18 (*a*). A plot of the resistance change vs

aging time showed the presence of maxima after short aging times at each of the three temperatures, Fig. 18 (*b*); the peaks shift to longer times for lower aging temperatures. With the precipitation of the α phase, the resistivity value decreased below the as-quenched value. This decrease in resistivity followed a sigmoidal variation with aging time, which is characteristic of phase transformation reactions involving nucleation and growth processes. Further, as the aging temperature was increased, the shape of the plot of resistivity vs aging time remained unaltered, but the curve itself was shifted to shorter times. The resistivity results are included here as supporting evidence for the clustering tendency in this alloy.

D) Hardness Measurements

Fig. 19 shows the variation of hardness of bulk specimens during isothermal aging treatments at 300°, 350°, 400°, 450°, and 500°C for periods up to 1000 hr following solution treatment at 800°C and a rapid quench in water. No significant increase in hardness was noticed during the initial stages of aging. The rapid increase in hardness which follows the initial stages occurs at times corresponding to the appearance of the α phase. Overaging does not occur up to 1000 hr at the lower aging temperatures, although it does occur after approximately 750 hr at 500°C. The heat treatment variables such as the solution treatment temperature and the cooling rate do not alter the hardness significantly during aging, Fig. 20.

DISCUSSION

The results of the present investigation show that the decomposition of the metastable β phase in the Ti-13V-11Cr-3Al alloy does not proceed through the precipitation of the transition phase ω as has been proposed by earlier investigators.[4,6,9] This result is not surprising since increasing additions of β-stabilizing elements to titanium have been found to retard the ω reaction. When present in sufficient amounts they have been found to suppress completely ω, and the observation that no ω phase appears in the ternary alloy Ti-13V-11Cr substantiates this argument. The aluminum addition is expected to inhibit ω formation further, since aluminum has been shown to be a strong suppressor of ω.[18,23]

All of the observations indicate that the decomposition of the metastable β in the present alloys at temperatures below ~550°C proceeds through a phase separation reaction leading to the formation of solute rich and solute lean phase, *i.e.*: $\beta_m \rightarrow \beta_{\text{rich}} + \beta_{\text{lean}}$.

Two aspects of the proposed reaction deserve particular attention: 1) the parent and the product phases are crystallographically identical, and they maintain a compositional difference, and 2) the new phase forms through a process involving nucleation and growth. The former of the two aspects suggests that it is possible to interpret the mode of decomposition with the aid of an inflected curve on a hypothetical free energy-composition diagram. The second aspect immediately implies that a spinodal type of decomposition mode is not probable although the composition of the parent phase might be within the miscibility region. Thus, the proposed phase separation should occur through stable composition fluctuations leading to the formation of

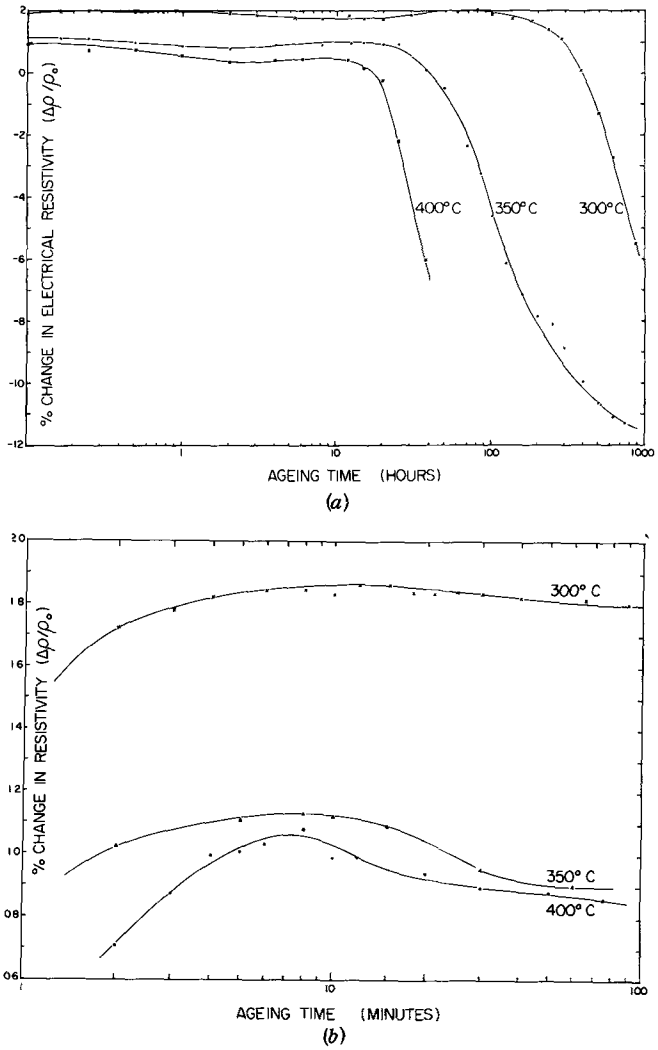

Fig. 18—(*a*) Changes in electrical resistivity as a function of time during isothermal aging of Ti-13V-11Cr-3Al alloy water quenched from 800°C. (*b*) Changes in electrical resistivity during the early stages of decomposition of the metastable β phase in Ti-13V-11Cr-3Al alloy water quenched from 800°C.

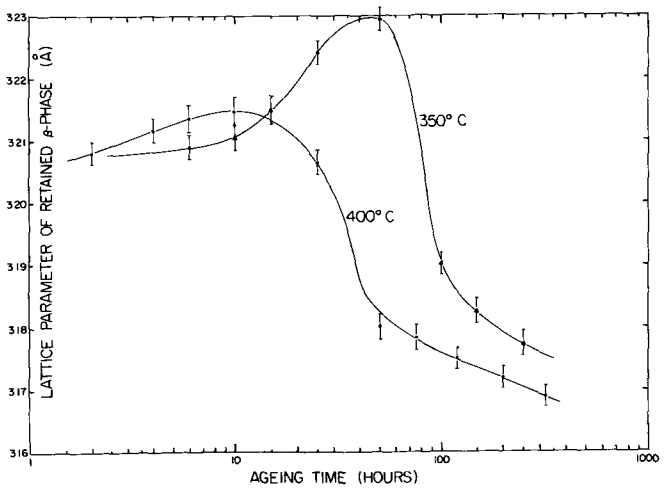

Fig. 17—Lattice parameter of the retained β phase as a function of aging time for Ti-13V-11Cr-3Al alloy.

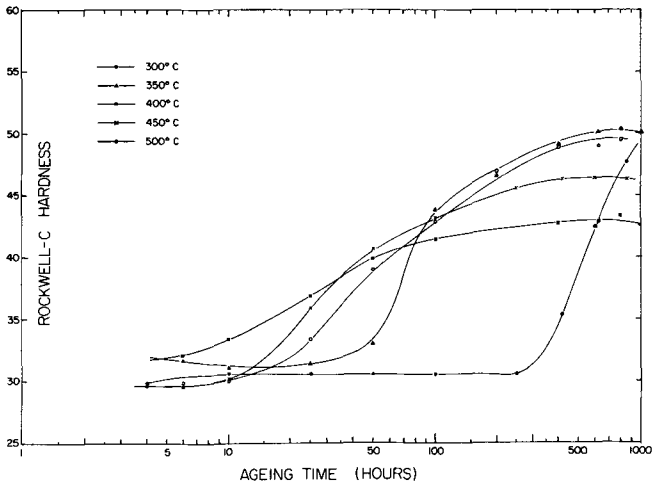

Fig. 19—Rockwell-C hardness vs aging time for Ti-13V-11Cr-3Al alloy, with aging temperature as a parameter.

stable solute rich regions which subsequently grow in size and alter in composition on continued aging, until the composition reaches the values determined by the common tangent condition. Since the decomposition of the metastable β probably proceeds by a diffusional clustering mechanism, the size and distribution of the particles of the product phase should reflect the influence of excess vacancies on the nucleation and growth process. A slower rate of quench yields a lower supersaturation of vacancies and hence an initial coarse distribution of clusters. Higher solution treatment temperatures and rapid quenches result in higher supersaturation of vacancies and a fine dispersion of clusters. Finally, for a given solution treatment temperature and quenching procedure, the supersaturation of vacancies as well as solute atoms will be higher for lower aging temperatures. As has been pointed out by Embury and Nicholson,[24] these two factors lead to a reduction in the critical nucleus size and the activation energy for nucleation and thus increases the probability of forming stable cluster nuclei. The result is a fine dispersion of precipitates. The present observations regarding the precipitate free zone, Figs. 10 and 11 (*e*), lend further evidence for the vacancy/solute atom model for the nucleation of the clusters. The fact that dislocations do not act as preferred nucleation sites for these clusters in rapidly quenched specimens suggests that excess vacancies provide easy nucleation conditions within the matrix.

The parent and product phases differ in their lattice parameters due to the compositional differences. Since the new phase attempts to maintain coherency with the matrix, an elastic energy term is introduced into the energetics of the reaction which is equal in magnitude to the reversible work necessary to match the lattices. An important outcome of this elastic anisotropy of the matrix influences the habit plane and morphology of the precipitate. The precipitate tends to follow elastically soft planes of the matrix, which for cubic crystals have been shown to be $\{100\}$ or $\{111\}$.[25] The $\{100\}_\beta$ habit observed in the current investigation is, therefore, in agreement with what would be expected from theory. The choice of the $\{100\}$ habit and coherent matching often distorts the precipitates giving the impression that they are slightly tetragonal.[25] This distortion may account for the plate-like or disc-shaped morphology observed in the present study.

The appropriate thermodynamic data required for a more complete prediction of the β transformation behavior in the Ti-V-Cr-Al system are not available. On the other hand, isothermal sections at 1000°C and 700°C for the ternary system Ti-V-Cr exhibit a pseudomiscibility gap which extends from the Ti-Cr binary into the ternary; this gap is wider at 700°C than at 1000°C.[26] A tendency toward phase separation may become increasingly pronounced at still lower temperatures to give rise to a metastable miscibility gap which is always below the equilibrium solubility surface. The proposed existence of such a gap is supported by the electron microscope studies of the decomposition behavior at 400°C of the Ti-13V-11Cr alloy whose composition lies just outside the ternary miscibility gap at 700°C. The observed occurrence of the phase separation reaction at 400°C suggests that the metastable miscibility gap in the ternary system expands as the temperature is lowered and that the composition of the alloy Ti-13V-11Cr lies within this gap at 400°C. Thus, at temperatures above ~550°C the composition of the present ternary alloy is probably outside a metastable miscibility gap. A similar gap should appear in the present quaternary system.

The initiation of the precipitation of the α-phase particles adjacent to β_2 precipitates or in regions between β_2 precipitates suggests that the β_2 is the solute rich bcc phase. The clustering of solute atoms also explains the initial increases in lattice parameter[27] and electrical resistivity.[29] With copious precipitation of α, the β_2 precipitates tend to vanish, which might be through either a redissolution process or by merging with the β matrix which becomes increasingly enriched with the precipitation of the α phase.

A comparison of the aging kinetics of the Ti-13V-11Cr and the Ti-13V-11Cr-3Al alloys suggests that the addition of aluminum to the ternary alloy tends to increase the aging response by accelerating the precipitation of the equilibrium α phase. The initial phase separation reaction, on the other hand, is retarded by the presence of aluminum.

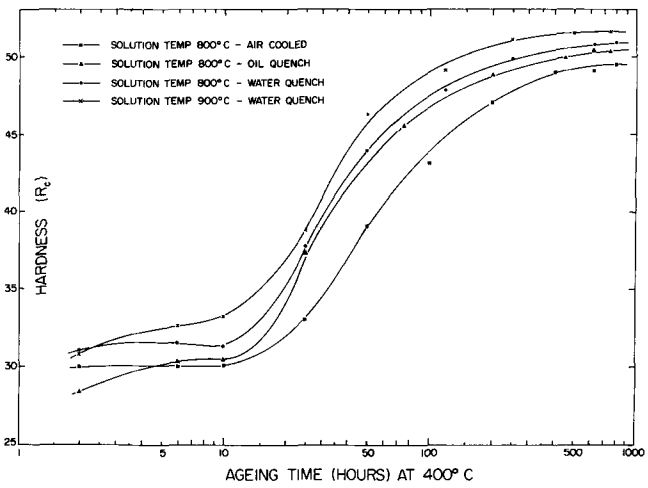

Fig. 20—Rockwell-C hardness vs aging time for Ti-13V-11Cr-3Al alloy with solution temperature and quench rate as variables.

Other workers have proposed that solute segregation or β-phase separation occurs during low temperature aging in Ti-16V-2.5Al,[18,29] Ti-8Al-1V-1Mo,[30] Ti-20V,[18] and Ti-9Mo-7Mn-(1 to 2)Al[19] alloys. Also, additional X-ray lines have been reported to be present near β-matrix reflections in Ti-Fe-Cr[28] and Ti-Cr[31] alloys. It is reasonable to believe that the decomposition mechanism presented here, based on the observations made on Ti-13V-11Cr and Ti-13V-11Cr-3Al alloys, may be expected in other titanium alloys when sufficient β stabilizing additions are present to retain β at room temperature. It can be shown by thermodynamic arguments[32] that the thermodynamic properties of a ternary solid solution A-B-C in the vicinity of one of the pure components, *e.g.* B, approach the weighted average of those properties exhibited by the binaries B-A and B-C. Thus, in the case of the Ti-13V-11Cr alloy, the observed tendency for demixing or phase separation should be a reflection of the tendencies exhibited by the binaries Ti-Cr and Ti-V. An examination of the thermodynamic data available in the literature for these systems sybstantiates the above argument. The activities of chromium and titanium in β-Ti-Cr solid solutions in the range 1250° to 1380°C[33] show a positive deviation from Raoult's law. The deviations become more significant as the temperature is lowered from 1380° to 1250°C. Recent superconducting measurements[34] of the low temperature phase transformations in Ti-Cr alloys with chromium contents >10 pct (by weight) show that compositional fluctuations in fact exist in this system. Krisement[35] has proposed a miscibility gap in the Ti-V binary system which is based on the positive heats of mixing of the β-Ti-V solid solutions. Thus, a tendency for clustering exists in both the Ti-Cr and the Ti-V binary systems although little experimental evidence is available at present.

CONCLUSIONS

1) The decomposition of the metastable β phase in Ti-13V-11Cr-3Al and Ti-13V-11Cr alloys at temperatures below ~500°C does not proceed through the precipitation of the transition phase ω.

2) However, in this temperature range, the supersaturated β phase undergoes a transition reaction leading to the formation of two bcc phases: a solute rich precipitate β_2 and a solute lean matrix β_1. The upper limit of the stability of β_2 phase is approximately 550°C.

3) The aluminum addition improves the aging response of the Ti-13V-11Cr alloy by accelerating the α precipitation reaction and retards the phase separation reaction.

4) Cold work prior to aging enhances the precipitation of α phase during subsequent aging, but it has little or no influence on the precipitation of β_2 phase.

ACKNOWLEDGMENT

This research was supported by the Advanced Research Projects Agency of the Department of Defense (ARPA Order 878) and was monitored by the Naval Research Laboratory under Contract No. N00014-66-C0365.

REFERENCES

1. M. K McQuillan: *Met. Rev.*, 1963, vol. 8, p. 41.
2. Iu A. Bagariatskii, G. I. Nosova, and T. V. Tagunova: *Soviet. Phys. Doklady*, 1959, no. 3, p. 1014
3. M. J. Blackburn and J C. Williams: *Trans. TMS-AIME*, 1968, vol. 242, p. 2461.
4. R. A. Wood and H. R Ogden: All-Beta Titanium Alloy Ti-13V-11Cr-3Al, 1959, DMIC Report 110.
5. A. G Imgram, D. N. Williams, and H. R. Ogden *Trans. TMS-AIME*, 1963, vol 227, p. 743.
6. R. A. Rowe, J. M. Dupouy, and M B. Bever: *Trans. TMS-AIME*, 1960, vol. 218, p. 821.
7. L. E. Tanner: *Trans. ASM*, 1961, vol 53, p. 407.
8. J. F. Rudy, F. A. Crossley, and H Schwartzbarf: *Welding J*, 1961, vol. 40, pp 447-S.
9. L E. Tanner and J. E. Coyne. *J Metals*, 1961, vol. 13, p 683
10. P. B Hirsch, A. Howie, R. B. Nicholson, D. W. Pashley, and M. J. Whelan: *Electron Microscopy of Thin Crystals*, 1st ed., pp. 32-34, New York Plenum Press, London, 1965.
11. M J. Blackburn and J. C. Williams. *Trans. TMS-AIME*, 1967, vol. 239, p. 287.
12. R. H Ericksen, R. Taggart, and D. H. Polonis: *Trans. TMS-AIME*, 1967, vol. 239, p. 236.
13. J. C Williams and M. J. Blackburn: *Trans. ASM*, 1967, vol. 60, p. 373
14. R. H Ericksen, R Taggart, and D. H. Polonis: *Trans. TMS-AIME*, 1969, vol 245, p. 359.
15. K G McIntyre and L. M. Brown: *J. Physique*, Supplement to No. 7-8, 1966, vol 27, pp C3-178.
16. G Thomas: *Trans. TMS-AIME*, 1965, vol. 233, p. 1608.
17. L. I van Torne and G. Thomas: *Acta Met.*, 1966, vol. 14, p. 621
18. E L. Harmon and A. R. Troiano *Trans. ASM*, 1961, vol. 53, p. 43.
19. N. V. Ageyev and P. K. Novik: *Russian Metallurgy*, 1965, no. 5, p. 46.
20. C Panseri and T. Federighi: *Acta Met.*, 1960, vol. 8, p 217.
21. A Kelly and R B. Nicholson. *Prog. Mater. Sci.*, 1963, vol. 10, p. 149.
22. P. Wilkes: *Acta Met.*, 1968, vol. 16, p. 683.
23. V. H. Weigand and H. G. Dorst: *Z. Metallk.*, 1965, vol. 56, p. 114.
24. J. D. Embury and R. B. Nicholson: *Acta Met.*, 1965, vol 13, p. 403
25. J. W. Cahn. *Trans. TMS-AIME*, 1968, vol. 242, p. 166.
26. P. A. Farrar and H. Margolin *Trans ASM*, 1967, vol. 60, p. 57.
27. S. E. Naess: *Scripta Met.*, 1969, vol 3, p 179.
28. N. V Ageev, Aginski, and L. A Petrova. *Izv. Zn SSSR Otn, Metallurgiya i Toplivo*, 1961, no. 5, p. 86.
29. L. E. Tanner: *Trans. TMS-AIME*, 1961, vol. 221, p 74.
30. M. J. Blackburn *Trans. ASM*, 1966, vol. 59, p. 694.
31. Iu. Bagaryatskii and G. I. Nosova. *Russian Metallurgy and Fuels*, 1962, no. 4, p. 116.
32. D. Y. Lee: M.S. Thesis, University of Washington, 1967.
33. M. J. Pool, R. Speiser, and G R. St. Pierre: *Trans. TMS-AIME*, 1967, vol. 239, p. 1180.
34. T. S. Luhman, R. Taggart, and D H Polonis: *Scripta Met*, 1969, vol. 3, p. 777.
35. Otto Krisement: *Z. Metallk.*, 1961, vol. 52, p. 695.